

High PD-L1 expression drives glycolysis via an Akt/mTOR/HIF-1 α axis in acute myeloid leukemia

PING MA^{1*}, MENGTAO XING^{2*}, LIJIE HAN¹, SILIN GAN¹, JIE MA¹, FEIFEI WU¹, YUMIN HUANG¹,
YANLI CHEN¹, WENLIANG TIAN¹, CHAO AN¹, HUI SUN¹ and LING SUN¹

¹Department of Hematology, The First Affiliated Hospital of Zhengzhou University, Zhengzhou, Henan 450052, P.R. China;

²Department of Biological Sciences, University of Texas at El Paso, El Paso, TX 79902, USA

Received September 23, 2019; Accepted December 19, 2019

DOI: 10.3892/or.2020.7477

Abstract. Acute myeloid leukemia (AML) is a hematological malignancy derived from immature myeloid cells, which have the characteristics of abnormal proliferation and differentiation. Glycolysis has been a popular topic of research in recent years, with increasing uptake and consumption of glucose. The present study aimed to investigate the glycolysis of tumor cells in patients with AML; in particular, how programmed cell death 1 ligand 1 (PD-L1) regulates tumor cells glycolysis using real time PCR (RT-PCR), western blotting and flow cytometry. PD-L1 high expression predicted poor outcome in patients with AML in the public database Gene Expression Profiling Interactive Analysis. PD-L1 expression was decreased in the samples from patients with AML with complete remission compared to that in patients with relapsed or refractory AML. In AML cell lines, glycolysis-associated genes ALDOA, PGK1, LDHA and HK2 were highly expressed in a PD-L1 high-expressed cell line. Overexpressed PD-L1 enhanced glucose consumption and the extracellular acidification rate, accompanied by decreased apoptosis and accumulation of cells in the S phase. In contrast, the apoptosis rate of tumor cells and the percentage of cells in the S phase were significantly

increased following PD-L1 knockdown in the THP1 cell line. HK2 and LDHA expression decreased after AML tumor cells were treated with Akt inhibitor or rapamycin. In addition, the PD-L1-overexpressed cell line (PD-L1-OV) MOLM-13 exhibited rapid tumor progression. Glycolysis-associated genes were highly expressed in tumor tissues of PD-L1-OV MOLM-13, with increased Ki67. Based on these findings, PD-L1 may be considered as a suitable marker for prognosis and treatment in the clinical setting.

Introduction

Acute myeloid leukemia (AML) is a complex and common myeloid malignancy, which is accompanied by the abnormal proliferation and differentiation of bone marrow precursor cells in the hematopoietic system (1,2). At the present stage, older adults with this disease have a worse prognosis (3). In addition, although certain patients may attain complete remission, it is easy to relapse (4). In recent years, second generation sequencing technology has been widely used in the clinic to aid diagnosis (5). For example, NPM1 and CEBPA mutations are favorable for clinical prognosis, but certain gene mutations are associated with poor outcomes for patients with AML, such as ACTN, TET2 and RUNX1 (5-7). However, it is essential to identify novel and effective targets for clinical treatment. To further investigate the mechanism underlying AML development, it is essential to better understand this disease and thus find new therapeutic targets.

Immune checkpoint blockades, such as cytotoxic T-lymphocyte-associated protein 4 (CTLA4) and programmed death 1 (PD-1), have been widely used for different types of cancer (8). Programmed cell death 1 ligand 1 (PD-L1) is one of the ligands of PD-1, binding to PD-1 to inhibit activated T-cell function (9). A large body of evidence has demonstrated that PD-L1 was positively associated with immune system suppression and tumor progression. High expression of PD-L1 was significantly associated with lower tumor-associated antigen distribution and clinical recurrence in patients with prostate cancer (10). PD-L1 expression in tumor cells could protect those cells from interferon (IFN) impairment, and the IFN signaling pathway was inhibited by PD-L1 (11). Bertucci *et al* also demonstrated that metastatic relapse in patients with soft-tissue sarcomas were strongly associated

Correspondence to: Professor Ling Sun, Department of Hematology, The First Affiliated Hospital of Zhengzhou University, 1 Jianshe Road, Zhengzhou, Henan 450052, P.R. China
E-mail: sunling6686@126.com

*Contributed equally

Abbreviations: AML, acute myeloid leukemia; CTLA4, cytotoxic T-lymphocyte-associated protein 4; PD-1, programmed death 1; PD-L1, programmed cell death 1 ligand 1; IFN, interferon; TIGAR, TP53-induced glycolysis and apoptosis regulator; BMMCs, bone marrow mononuclear cells; PBS, phosphate-buffered saline; RT-PCR, real time PCR; FBS, fetal bovine serum; PD-L1-OV, PD-L1 overexpressed; ECAR, extracellular acidification rate; IHC, immunohistochemistry

Key words: programmed cell death 1 ligand 1, glycolysis, acute myeloid leukemia, metabolism, signaling pathway

with PD-L1 expression (12). Following treatment with IFN- γ , PDL1 expression was upregulated in myeloid leukemia cell lines via the STAT3 pathway (13). In symptomatic multiple myeloma, PD-L1 expression in plasma cells was closely associated with cancer progression (14). PD-L1 had been used as a therapeutic target for various different types of cancer treatment (15). Therefore, it is essential to research the impact of PD-L1 expression in patients with AML.

In recent years, tumor cell metabolism has been a popular topic for research, with several hallmarks including increasing the uptake of glucose, amino acids and nitrogen, alteration of metabolite-associated genes, and the interaction between metabolites and the tumor microenvironment (16). Mitochondrial ROS in primary AML cells induced by drugs could be inhibited by SIRT3, a SOD2 deacetylase, which could also protect AML cells from chemokine-induced apoptosis (17). AML cells exhibited high metabolism of the amino acid glutamine for longer survival, and inhibiting this pathway induced AML cell apoptosis (18). Although the cytoplasmic tail of PD-L1 is too short to find evident signaling motifs, certain studies have still reported that PD-L1 could induce cell signaling activation in tumor cells, such as signaling from PD-1 toward PD-L1 (19). PD-L1⁺ tumor cells resisted apoptosis induced by the Fas-Fas ligand pathway or cytokines secreted by T cells (20). It has been reported that PD-L1-expressing tumor cells triggered cell intrinsic glycolysis through the mTOR signaling pathway, which could enhance tumor growth and progression (21). Currently, it is unclear whether PD-L1 expressed in AML cells enhances cell glycolysis or inhibits tumor cell apoptosis.

Poulain *et al* demonstrated that AML cells exhibited high uptake of glucose, strong glycolysis ability and overactivated mTOR signaling (22). The TP53-induced glycolysis and apoptosis regulator (TIGAR) was highly expressed in patients with cytogenetically normal AML, and knockdown of TIGAR promoted tumor cell apoptosis and enhanced the sensitivity of tumor cells to glycolysis inhibitor (23). Cascone *et al* demonstrated that glycolysis-associated genes included HK2, LDHA, ALDOA, ALDOC, ENO2 and PGK1 (24). It has also been revealed that Glut1, associated with glycolysis, was regulated by the PI3K/Akt/mTOR signaling pathway (19). Despite glycolysis having been demonstrated in AML cells, the effects of PD-L1 on glycolysis in patients with AML remain largely unknown. The present study primarily investigated how PD-L1 regulates tumor cell glycolysis. First, the present study collected AML patient samples and revealed that PD-L1 was positively correlated with glycolysis-associated genes (HK2, PFKM, ALDOA, PGK1, PDK1 and LDHA). Overexpressed PD-L1 in AML cell line MOLM-13 significantly upregulated the expression of glycolysis-associated genes via the AKT/mTOR signaling pathway, and downregulated tumor cell apoptosis *in vitro*, indicating that PD-L1 could regulate tumor cell metabolism and proliferation without PD-1 existence.

Materials and methods

Patients and ethical statement. The present study included 90 patients (52 males and 38 females; age range, 14–81 years) that had been newly diagnosed with AML without any other disease from the First Affiliated Hospital of Zhengzhou University during January 2016 and May 2019. All patients provided

written informed consent. Ethical approval was obtained from the Human Research Ethics Committee (First Affiliated Hospital of Zhengzhou University, China). The database GEPIA (<http://gepia.cancer-pku.cn/>) was used for survival analysis and correlation analysis in TCGA database of AML.

RNA extraction. Bone marrow mononuclear cells (BMMCs) were obtained from patients and healthy donors through density gradient centrifugation. BMMCs were washed with phosphate-buffered solution (PBS) two times and 1 ml TRIzol (Takara Bio, Inc.) was added. Chloroform was added to the TRIzol and mixed immediately. After 10 min, BMMCs were centrifuged for 10 min at 13,500 \times g. The upper transparent supernatant was isolated and mixed with isopropanol in new tubes without RNase. This mixture was then centrifuged for 10 min at 13,500 \times g. The white sediment was the separated RNA. A total of 75% absolute ethyl alcohol were used to wash the RNA twice. RNAs were stored in an ultra-low temperature freezer.

Synthesis of cDNA and real time PCR (RT-PCR). cDNA was synthesized using a PrimeScript RT reagent kit and a gDNA Eraser kit (Perfect Real Time; Takara Bio, Inc.) according to the manufacturer's protocol. In general, 1 μ g RNA was used for the cDNA synthesis. An equal amount of cDNA was used as templates for RT-PCR to detect gene expression. The reaction system included 2 μ l diluted cDNA, 10 μ l SYBR Premix Ex Taq (Takara Bio, Inc.) and 1 μ M primer forward and reverse. Finally, water was added to reach a final volume of 20 μ l. Primers used for PCR were synthesized by Sangon Biotech (Shanghai) Co., Ltd., and their sequences are presented in Table S1. The thermocycling conditions for each reaction included an initial hold at 95°C for 30 sec, followed by 40 denaturation cycles at 95°C for 5 sec and annealing/extension at 60°C for 30 sec. CFX96 Touch Real-Time PCR Detection System (Bio-Rad Laboratories, Inc.) was used for the RT-PCR amplification. Finally, the relative level of each gene expression was calculated using the $2^{-\Delta\Delta C_q}$ method (25).

Cell culture, lentivirus package and infection. AML tumor cell lines HL-60 and KG-1a (American Type Culture Collection) were cultured in Iscove's Modified Dulbecco's Medium (Thermo Fisher Scientific, Inc.) with 10% fetal bovine serum (FBS; Thermo Fisher Scientific, Inc.) at 37°C in an incubator with 5% CO₂. MOLM-13 and THP1 cells lines were cultured in RPMI-1640 medium (Thermo Fisher Scientific, Inc.) with 10% FBS at 37°C in an incubator with 5% CO₂.

To induce overexpression and knockdown of PD-L1 in cells, a FUA-CMSZ-GFP vector containing PD-L1 full length, and GV493-GFP vector containing PD-L1 sh1/sh2 sequences were constructed. An empty vector served as the negative control. 293T cells were cultured in 6-well plates to transfect PD-L1 overexpressed (PD-L1-OV) vector or PD-L1-sh1/2 vector with package vector using Lipofectamine™ 3000 Transfection reagent (Thermo Fisher Scientific, Inc.) according to the manufacturer's protocol. Lentiviruses were obtained after 3–7 days and stored in an ultra-low temperature freezer for follow-up experiments. Lentivirus of PD-L1-OV or PD-L1-sh1/2 were also used to infect cell lines MOLM-13 and THP1 using Lipofectamine™ 3000.

Protein extraction and western blotting. AML cell lines MOLM-13 or THP1 were lysed with RIPA lysis buffer containing 1 mM PMSF (both from Beyotime Institute of Biotechnology). BCA assay method was used to detect the concentration of protein. Proteins (30 μ g per 20 μ l) were separated via SDS-PAGE (10% gel) at 80 V for 2 h, and then transferred to polyvinylidene fluoride membranes (Merck Millipore) at 200 mA for 2 h. 10% skim milk powder were incubated with protein at room temperature for 2 h. The antibodies of glycolysis-associated proteins HK2 (product code ab37593; dilution 1:500) and LDHA (product code ab125683; dilution 1:1,000; both from Abcam), PD-L1 antibody (product no. 13684; dilution 1:1,000; Cell Signaling Technology, Inc.), HIF-1 α antibody (product code H1 α 67; dilution 1:1,000; Abcam), AKT (catalog no. 60203-2-Ig; dilution 1:2,000; ProteinTech Group, Inc.)/p-AKT antibody (product code ab78403; dilution 1:2,000; Abcam), S6 (product no. 2217; dilution 1:1,000; pS6 antibody (product no. 4858; dilution 1:2,000; both from Cell Signaling Technology, Inc.) and β -actin (product no. 3700; dilution 1:4,000; Cell Signaling Technology, Inc.) were used as primary antibodies at 4°C overnight. In addition, the secondary antibodies included anti-mouse IgG (product code ab6728; dilution 1:5,000) and anti-rabbit IgG (product code ab6721; dilution 1:5,000; both from Abcam) which were incubated with proteins at room temperature for 1 h following incubation of the primary antibodies. Enhanced chemiluminescence (ECL) reaction (Thermo Fisher Scientific, Inc.) was used to detect protein bands and staining intensity was analyzed with software AI600 control (version 1.2.0; GE Healthcare, Inc.).

Cell apoptosis, proliferation and cell cycle detection. MOLM-13 (Blank, NC, PD-L1-OV; 1×10^6) and THP1 (NC, PD-L1-sh1/sh2; 1×10^6) were obtained from 6-well plates, and the cell cycle and apoptosis rate were detected using an Annexin V-FITC/PI Apoptosis Detection kit (Beijing Solarbio Science & Technology Co., Ltd.) and a Cell Cycle and Apoptosis Analysis Kit (Beyotime Institute of Biotechnology), respectively. BD FACSCanto™ II (BD Biosciences) was used to analyze data. In addition, the MOLM-13 (Blank, NC, PD-L1-OV; 1×10^6) cell line was cultured in 96-well plates for 1, 2, 3, 4 and 5 days to detect cell proliferation using a CCK-8 assay.

Glucose consumption assay. Tumor cells (Blank, NC and PD-L1-OV) were cultured in 6-well plates for 24 h, and the supernatants were collected for testing the glucose consumption with a Glucose Assay kit (Sigma-Aldrich; Merck KGaA).

Metabolism assay. The extracellular acidification rate (ECAR) was measured using a Seahorse XF Glycolysis Stress Test kit and Seahorse XF96 Extracellular Flux Analyzers (both from Agilent Technologies, Inc.). The data were analyzed and exported from Wave software (version 2.3.0.19; Agilent).

Immunohistochemistry (IHC) staining. Tumor tissues from mice were fixed with 4% paraformaldehyde at room temperature for 30 min and embedded in paraffin for protein detection. First, paraffin-embedded tumor tissues were

dewaxed at 65°C for 30-60 min. Citrate buffer was used for antigen retrieval using boiling water for 20 min. Nonspecific blockage solution and 3% hydrogen peroxide was added on the paraffin-embedded tumor tissues for blocking endogenous peroxidase and nonspecific antigen after the tissues cooled to the room temperature. Then, antibodies of glycolysis-associated protein LDHA (product code ab125683) and Ki67 (product code ab15580; both from Abcam) were stained at 4°C overnight. The next day, horseradish peroxidase-labeled rabbit anti-mouse (product code ab6728; dilution 1:200)/goat anti-rabbit (product no. 2217; dilution 1:500; both from Abcam) secondary antibody was added for the interaction with 3,3'-diaminobenzidine. Nuclear staining was performed using hematoxylin. Finally, paraffin-embedded tumor tissues were dehydrated and mounted by Permount™ Mounting medium.

Mouse experiment. The 5-6-week-old female NOD/SCID mice (NOD. CB17-Prkdcscid/NcrCrl) were obtained from Beijing Vital River Laboratory Animal Technology Co., Ltd. The formation of tumors were carried out as described in a previous study (26). The mice were randomly assigned into two groups [NC (n=5) and PD-L1-OV (n=5)]. The mice were euthanized with 1% pentobarbital sodium (150 mg/kg of body weight) by i.p. injection after the maximum diameter exceeded 2 cm during tumor growth. A density of 5×10^6 PD-L1-OV MOLM-13 and NC MOLM-13 cells were re-suspended into 100 μ l PBS and injected subcutaneously into the right flank of each mouse. The tumor volume and mouse weight were measured at 8, 13 and 18 days. Eighteen days after tumor formation, the mice with tumors were sacrificed in general in 150 mg/kg of body weight with 1% pentobarbital sodium through intraperitoneal injection and the animals were considered dead upon cardiac arrest. The mouse experiments were approved by the Institutional Animal Care and Use Committee of the First Affiliated Hospital of Zhengzhou University.

Statistical analysis. Analysis of the data was performed using SPSS Statistics 16.0 (SPSS, Inc.) and GraphPad Prism software 7.0 (GraphPad Software, Inc.). $P < 0.05$ was considered to indicate a statistically significant result. The results are expressed as the mean \pm standard error. Statistical significance was determined via one-way ANOVA, two-way ANOVA, Tukey's multiple comparisons test or unpaired Student's t-test. Pearson's χ^2 test was used to analyze the relationships between PD-L1 and glycolysis-associated genes.

Results

PD-L1 expression is associated with glycolysis and prognosis in patients with AML. A total of 90 patient samples, that had been newly diagnosed with AML, were collected and divided into two groups according to the expression of PD-L1. The clinical characteristics of these patients are presented in Table I. The present study first analyzed the association between PD-L1 and prognosis in the public database GEPIA (<http://gepia.cancer-pku.cn/>) based on cut-off-high (70%) and cut-off-low (30%) expression (27). Samples with an expression level $>70\%$ were considered as the high-expression cohort; conversely, samples with an expression level $<30\%$ were

Table I. Clinical characteristics in AML patients.

Characteristics	Total	PD-L1 expression	
		High	Low
Age/years, median (range)	43.5 (14-81)	48 (14-76)	42 (16-81)
Age group/n (%)			
≥60 years	16 (17.8)	9 (10)	10 (11.1)
<60 years	74 (82.2)	36 (40)	35 (38.9)
Sex/n (%)			
Male	52 (57.8)	28 (62.2)	24 (53.3)
Female	38 (42.2)	17 (37.8)	21 (46.7)
WBC/ x 10 ⁹ /l, median (range)	17.1 (1.1-350.3)	13.6 (1.1-350)	39.4 (1.34-229)
BM blasts/%, median (range)	64.6 (20-99.6)	57.6 (22.3-99.6)	66 (20-94.8)
PB blasts/%, median (range)	38.5 (0-98)	50 (0-97)	38 (0-98)
FAB subtypes/n (%)			
M0	3 (3.3)	2 (4.4)	1 (2.2)
M1	3 (3.3)	2 (4.4)	1 (2.2)
M2	43 (47.8)	20 (44.4)	23 (51.1)
M4	13 (14.4)	6 (13.3)	7 (15.6)
M5	25 (27.8)	13 (28.9)	12 (26.7)
M6	2 (2.2)	2 (4.4)	0 (0)
M7	1 (1.1)	0 (0)	1 (2.2)
Risk/n (%)			
Good	14 (15.6)	3 (6.7)	11 (24.4)
Intermediate	47 (52.2)	26 (57.8)	21 (46.7)
Poor	28 (31.1)	19 (42.2)	9 (20)
Cytogenetics/n (%)			
Normal	42 (46.7)	19 (42.2)	23 (51.1)
Complex	6 (6.7)	1 (2.2)	5 (11.1)
inv(16)/CBFβ-MYH11	9 (10)	2 (4.4)	7 (15.6)
t(8;21)/RUNX1-RUNX1T1	9 (10)	2 (4.4)	7 (15.6)
11q23/MLL	2 (2.2)	2 (4.4)	0 (0)
-7/7q-	5 (5.6)	3 (6.7)	2 (4.4)
t(9;22)/BCR-ABL1	2 (2.2)	2 (4.4)	3 (6.7)
Others	15 (16.7)	9 (20)	6 (13.3)

AML, acute myeloid leukemia; PD-L1, programmed cell death 1 ligand 1; WBC, white blood cell; BM, bone marrow; PB, peripheral blood; FAB, french american britain.

considered as the low-expression cohort. The results revealed that high PD-L1 expression predicted poor outcome in patients with AML (Fig. 1A). The 90 patients with AML were classified into a complete remission group and a relapsed or refractory group according to the clinical therapy responses. PD-L1 expression was decreased in patients with AML with complete remission compared with that in patients with relapsed or refractory AML (Fig. 1B), which was consistent with the results in the public database. Several studies have indicated that PD-L1 could promote glycolysis in other types of cancer (19). The present study observed a moderately positive correlation of PD-L1 expression with rate-limiting enzymes (HK2 and PFKM) in glycolysis (Fig. 1C). However, PD-L1 also exhibited a moderately positive correlation with

other glycolysis-associated enzymes, including ALDOA, PGK1, PDK1 and LDHA (Fig. 1D). It was demonstrated that PD-L1 was correlated with PDK1 and PFKM in GEPIA (Fig. S1A and B).

High PD-L1 expression in AML cell lines exhibits strong glycolysis ability. In order to better investigate the effect of PD-L1 expression, the present study selected four AML cell lines, HL-60, MOLM-13, KG-1a and THP1. First, the present study detected PD-L1 expression through RT-PCR and flow cytometry. The THP1 cell line exhibited the highest PD-L1 expression at both the mRNA level (F=107.5) and protein level (Fig. 2A and B). The present study also revealed that the expression levels of HK2 (F=254.5), ALDOA (F=213.5),

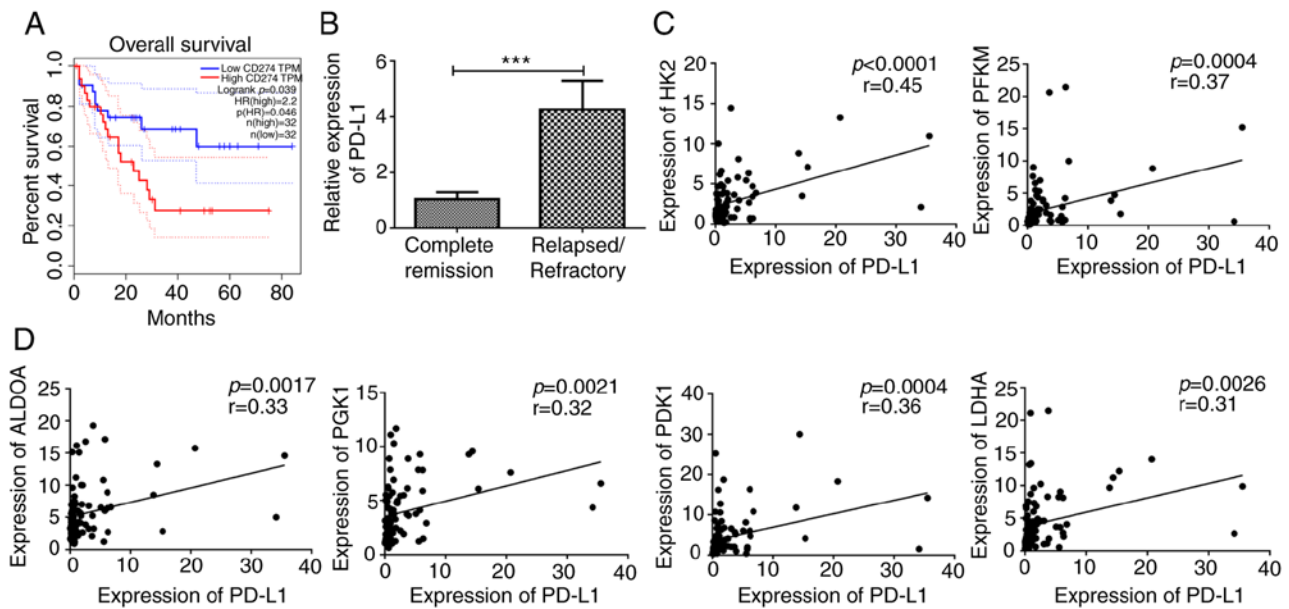


Figure 1. High PD-L1 expression represents poor prognosis and strong glycolysis metabolism in patients with AML. (A) Survival analysis of PD-L1 and prognosis in GEPIA. The dotted lines represent the 95% confidence interval information. BMMCs were obtained from patients with AML and used to detect gene expression. (B) PD-L1 expression was detected in 90 patients newly diagnosed with AML with complete remission and relapsed or refractory; the correlation between PD-L1 and glycolysis-associated genes (C) HK2 and PFKM, and (D) ALDOA, PGK1, PDK1 and LDHA in 90 patients with AML. *** $P < 0.001$. PD-L1, programmed cell death 1 ligand 1; AML, acute myeloid leukemia; BMMCs, bone marrow mononuclear cells.

PGK1 ($F=189.2$) and LDHA ($F=52.3$) were highly expressed in the PD-L1-high expressed cell line, THP1, indicating that PD-L1 may control cell glycolysis (Fig. 2C).

Overexpressed PD-L1 enhances cell glycolysis. In the present study, the PD-L1-OV MOLM-13 cell line was first obtained by infection. PD-L1 was successfully expressed in the PD-L1-OV MOLM-13 cell line ($F=36$) (Fig. 3A and B). Glycolysis-associated genes of PD-L1-OV MOLM-13 were assessed. HK2 ($F=91.04$), ALDOA ($F=24.53$), PGK1 ($F=31.16$) and LDHA ($F=37.11$) were highly expressed at the mRNA level in PD-L1-OV MOLM-13 cells compared to the blank and NC groups (Fig. 3C). HK2 is an important rate-limiting enzyme in glycolysis and LDHA mainly catalyzes lactic acid. To further confirm the change of HK2 and LDHA, the present study determined that the protein level of HK2 and LDHA was significantly increased in PD-L1-OV MOLM-13 cells (Fig. 3D). Due to the changes in these enzymes, the glucose consumption of PD-L1-OV MOLM-13 cells was enhanced ($F=69.29$) (Fig. 3E). In addition, PD-L1-OV MOLM-13 cells exhibited a higher level of ECAR, which could represent the glycolysis (Fig. 3F). PD-L1 expression of THP1 was knocked-down ($F=794.9$) (Fig. S2A and B), with a decrease of glycolysis-associated enzymes (HK2, $F=135.9$; ALDOA, $F=361.8$; PGK1, $F=58.73$; LDHA, $F=89.63$) (Fig. S2C and D).

PD-L1 inhibits tumor cell apoptosis and promotes tumor cells into the S phase. A previous study demonstrated that glycolysis could affect cell proliferation and apoptosis (28). Therefore, the proliferation of PD-L1-OV MOLM-13 cells was enhanced and verified using a CCK-8 assay (Fig. S3). Furthermore, the apoptosis rate of PD-L1-OV MOLM-13 cells exhibited a significantly decreasing trend ($F=98.28$) (Fig. 4A). The process of cell proliferation can be classified into three phases:

G_0/G_1 , S and G_2/M (29). PD-L1 promoted tumor cells into the S phase ($F=13.59$), indicating that PD-L1 could promote cell cycle progression (Fig. 4B). Conversely, the apoptosis of tumor cells ($F=466.5$) was significantly increased and the percentage of cells in the S phase ($F=14.02$) was significantly decreased following PD-L1 knockdown in the THP1 cell line (Fig. 4C and D), with a number of cells remaining in the G_0/G_1 phase.

PD-L1 promotes tumor cell glycolysis through AKT/mTOR/HIF-1 α signaling. PD-L1 has been reported to trigger the mTOR signaling pathway in a mouse sarcoma model (21). Hypoxia is a major characteristic in the bone marrow microenvironment (30). S6 was reported as a downstream effector of mTOR signaling (31). The present study demonstrated that PD-L1 expression was positively correlated with HIF-1 α in 90 patients with AML (Fig. 5A). Furthermore, the present study demonstrated that the activation of the AKT/mTOR/HIF-1 α signaling pathway was different according to the PD-L1 expression in the 4 AML cell lines (Fig. 5B). In order to further examine the regulatory mechanism of PD-L1 it was observed that, phosphorylation of Akt ($F=9.485$) and S6 ($F=10.26$) and HIF-1 α ($F=30.2$) expression was increased after MOLM-13 tumor cells over-expressed PD-L1, while cleaved caspase-3 ($F=44.31$) was decreased (Fig. 5C and D). In contrast, the Akt/mTOR/HIF-1 α signaling pathway (p-AKT, $F=37.91$; p-S6, $F=39.84$; HIF-1 α $F=122.7$) was inactivated in PD-L1-sh1 and PD-L1-sh2 THP1 cells while cleaved caspase-3 was activated ($F=8.801$) (Fig. 5E and F).

As presented in Fig. 3C, HK2 and LDHA were the genes that exhibited the greatest change in PD-L1-OV MOLM-13 cells, thus, the present study speculated that these two genes may be the downstream target genes of AKT/mTOR/HIF-1 α

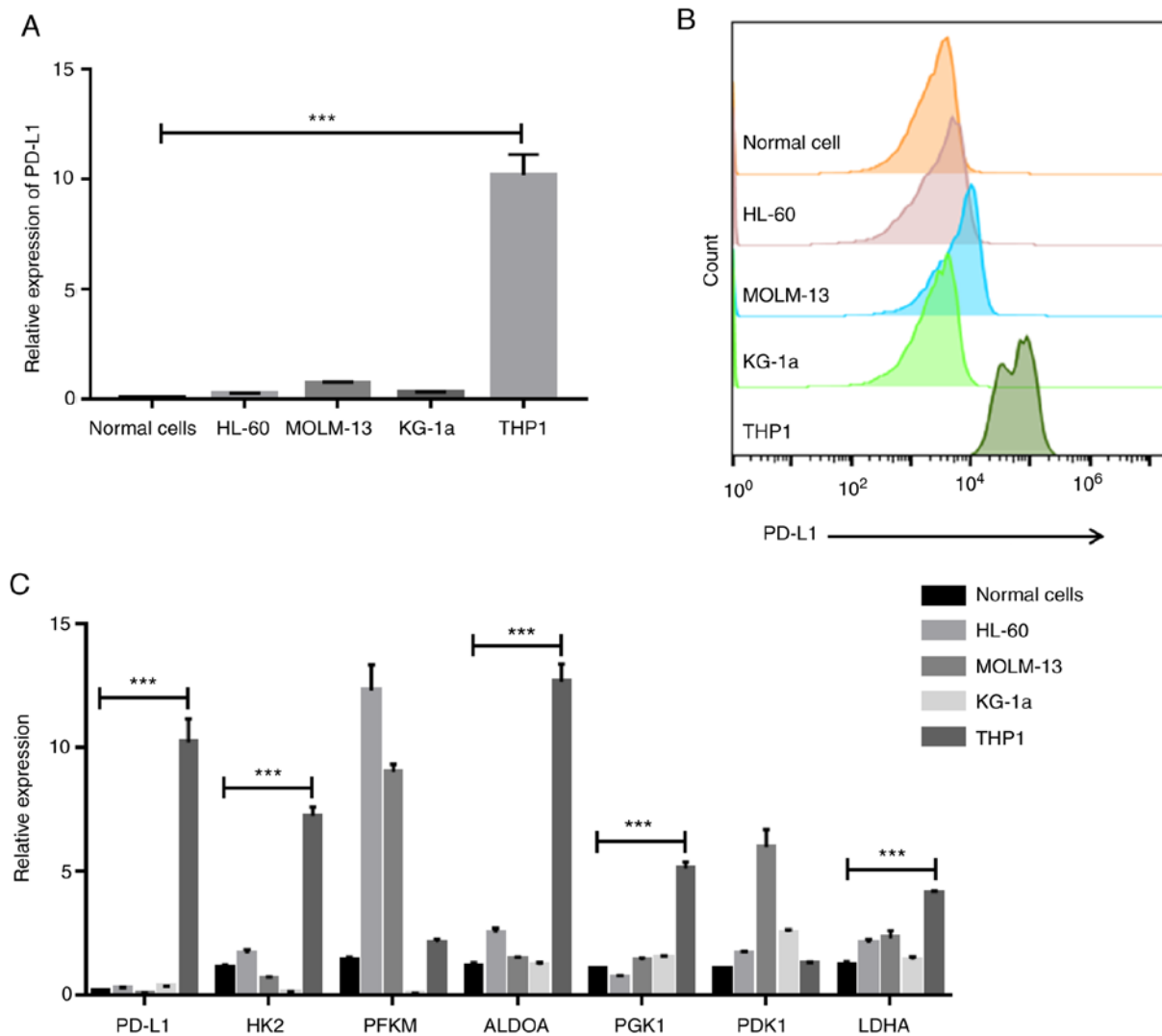


Figure 2. PD-L1 expression is positively associated with glycolysis in AML cell lines. Myeloid cells from healthy donors were harvested as negative controls. PD-L1 expression in normal cells and AML cell lines HL-60, MOLM-13, KG-1a and THP1 were detected by (A) RT-PCR and (B) flow cytometry. (C) Glycolysis-associated genes were also assessed by RT-PCR. Data represent the results obtained from three independent experiments. *** $P < 0.001$. PD-L1, programmed cell death 1 ligand 1; AML, acute myeloid leukemia.

signaling. The present study also demonstrated that phosphorylation of S6 and HIF-1 α expression were down-regulated concurrently following the phosphorylation of Akt via the Akt inhibitor (p-AKT, $F=6.227$; p-S6, $F=10.16$; HIF-1 α , $F=8.113$) (Fig. 6A and B). In addition, HK2 ($F=9.961$) and LDHA ($F=9.848$) expression was also significantly decreased in PD-L1-OV MOLM-13 cells treated with Akt inhibitor (Fig. 6A and B). In addition, rapamycin, an inhibitor of mTOR, was used to treat PD-L1-OV MOLM-13 cells to inhibit phosphorylation of S6. The expression of HK2 ($F=8.949$), LDHA ($F=7.811$) and HIF-1 α ($F=14.66$) was decreased in PD-L1-OV MOLM-13 treated with rapamycin compared to the PD-L1-OV MOLM-13 cells (Fig. 6C and D).

Overexpressed-PD-L1 promotes tumor growth in vivo. In order to confirm the proliferative effect of PD-L1 in AML cells *in vivo*, mouse models of PD-L1-OV MOLM-13 cells and NC were established in the present study. Tumor volumes of the PD-L1-OV MOLM-13 group were larger

at 8, 13 and 18 days compared with the NC MOLM-13 group (Fig. 7A). The images of the tumor size at 18 days also demonstrated the same result (Fig. 7B). Since it has been confirmed that the aforementioned glycolysis-associated genes were highly expressed in the PD-L1-OV MOLM-13 cell *in vitro* experiment, the genes were detected in tumor tissues. Glycolysis-associated genes and HIF-1 α were highly expressed in tumor tissues of the PD-L1-OV MOLM-13 group (Fig. 7C), and Ki67, a hallmark of proliferation, was increased in the PD-L1-OV MOLM-13 group (Fig. 7D). LDHA, regulated by PD-L1/AKT/mTOR, exhibited a highly expressed trend in tumor tissue of the PD-L1-OV MOLM-13 group (Fig. 7D). The data indicated that PD-L1 promoted AML cell proliferation by enhancing glycolysis.

Discussion

An increasing number of studies have demonstrated that cell metabolism adjusted AML cell occurrence and development.

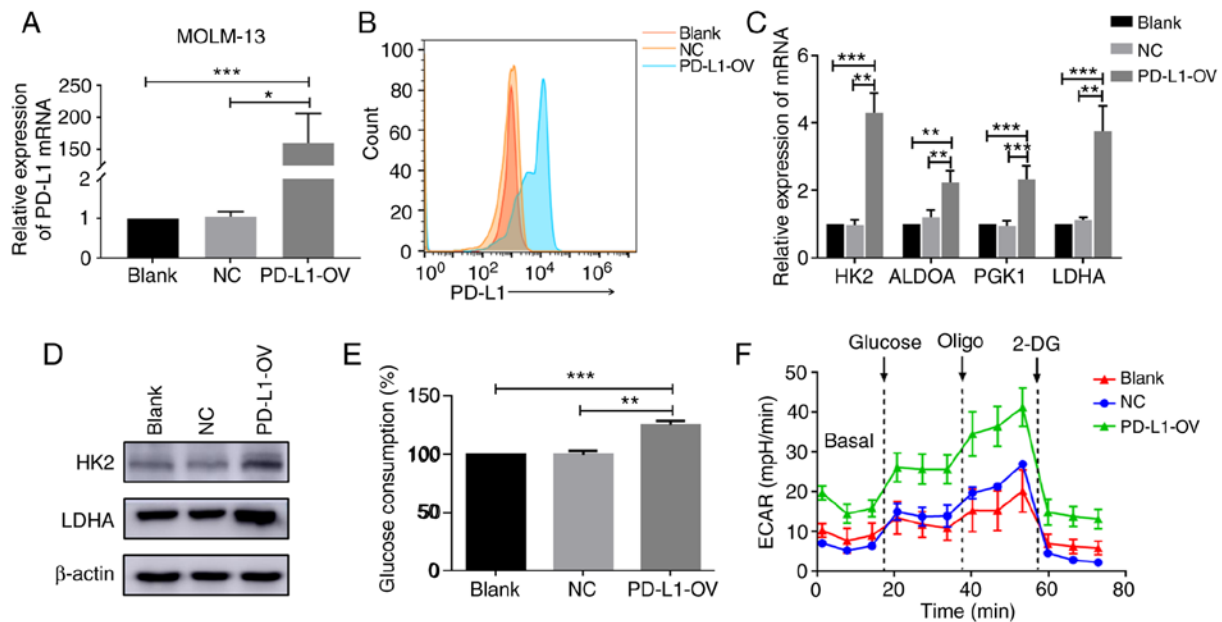


Figure 3. Glycolysis-associated genes are increased in PD-L1-OV MOLM-13 cells. MOLM-13 cells were infected with control lentivirus or PD-L1-OV lentivirus for 7 days and GFP⁺ tumor cells were selected by flow cytometry. PD-L1 expressed in MOLM-13 (blank), control lentivirus-infected MOLM-13 (NC) and PD-L1-OV lentivirus-infected MOLM-13 (PD-L1-OV) were assessed by (A) RT-PCR and (B) flow cytometry. (C) RT-PCR was used to detect glycolysis-associated genes in Blank, NC and PD-L1-OV MOLM-13 cells. (D) HK2 and LDHA expression were assessed via western blotting. (E) Tumor cells (Blank, NC and PD-L1-OV) were cultured in 6-well plates for 24 h and the supernatants were collected for glucose consumption detection. MOLM-13 and transfected MOLM-13 cells (NC and PD-L1-OV) were plated into 96-well plates and (F) ECAR was assessed after cells were cultured in a CO₂-free incubator for 1 h. Data represent the results obtained from three independent experiments. *P<0.05, **P<0.01 and ***P<0.001. PD-L1-OV, PD-L1 overexpressed; ECAR, extracellular acidification rate.

The notion that oxidative phosphorylation could result in chemotherapy-resistant and tumor progression in patients with AML has previously been verified (32,33). AML cell proliferation and stemness were regulated by phospholipid metabolism (34). The present study primarily focused on the association between PD-L1 and glycolysis in AML cells. Patients with AML who expressed high levels of PD-L1 exhibited an enhanced glycolysis ability. However, it was revealed that some patients with high levels of glycolysis gene expression exhibited low expression of PD-L1, the reason for this may be individual heterogeneity. Further assays were performed to investigate the correlations between PD-L1 and glycolysis in the present study. By overexpressing PD-L1 *in vitro*, it was revealed that the glycolysis-associated genes in tumor cells were upregulated, with increasing proliferation and decreasing apoptosis.

Mounting evidence has suggested that the glycolysis pathway is a potent target of cancer treatment. In pancreatic cancer, tumor cell invasion and metastasis could be promoted by glycolysis, which indicates that targeting glycolysis may be a new therapeutic approach (35). LDHA plays an important role in glycolysis, and inhibited LDHA-impacted tumor cell viability in both *in vivo* and *in vitro* preclinical models of Ewing sarcoma, accompanied by weakened glycolysis (36). HK2, known as a pivotal rate-limiting enzyme, mainly regulates cell glycolysis. Targeting HK2 with costunolide decreased the uptake of glucose and lactate accumulation, resulting in suppression of hepatic stellate cell viability, which is the major cell for hepatic fibrosis (37). It has been demonstrated that glycolysis metabolism was associated with tumor cell development and progression in oral tongue

squamous cell carcinomas (38). In the results of the present study, regardless of whether PD-L1 was overexpressed or knocked-down, the expression of HK2 and LDHA was increased or decreased in AML cells MOLM-13 with cell proliferation altered, which was consistent with the results observed in other tumor types (38). Several studies have reported the impact of glycolysis in AML. Inhibition of PDK promoted tumor cell apoptosis, and it has been demonstrated that PDK would be a poor prognostic marker in patients with AML through The Cancer Genome Atlas database (39). Song *et al* observed that glycolysis was associated with resistance to chemotherapy (40). Although glycolysis was researched in AML, the majority of studies only reported the phenomenon, without investigating the mechanism.

In breast cancer, PD-L1 could predict the outcome of patients (41). PD-L1 promoted tumor cell growth through mTOR signaling in head and neck squamous cell carcinoma carcinogenesis cell lines Cal-27 and Fadu (42). Consistent with these findings, the present study revealed that PD-L1 expression was decreased in patients with AML with complete remission compared with that in patients with relapsed or refractory in the 90 samples from patients with AML. In addition, PD-L1-OV MOLM-13 demonstrated increasing cell viability and decreasing apoptosis. Li *et al* demonstrated that MET downregulated PD-L1 expression by activating GSK3B. The invasion of liver cancer cells was increased after using the MET inhibitor (43). Icotinib increased the proliferation of hepatocellular carcinoma cell lines both *in vitro* and *in vivo* by upregulating PD-L1 expression; this phenomenon would be diminished when knocking-down PD-L1 expression in tumor

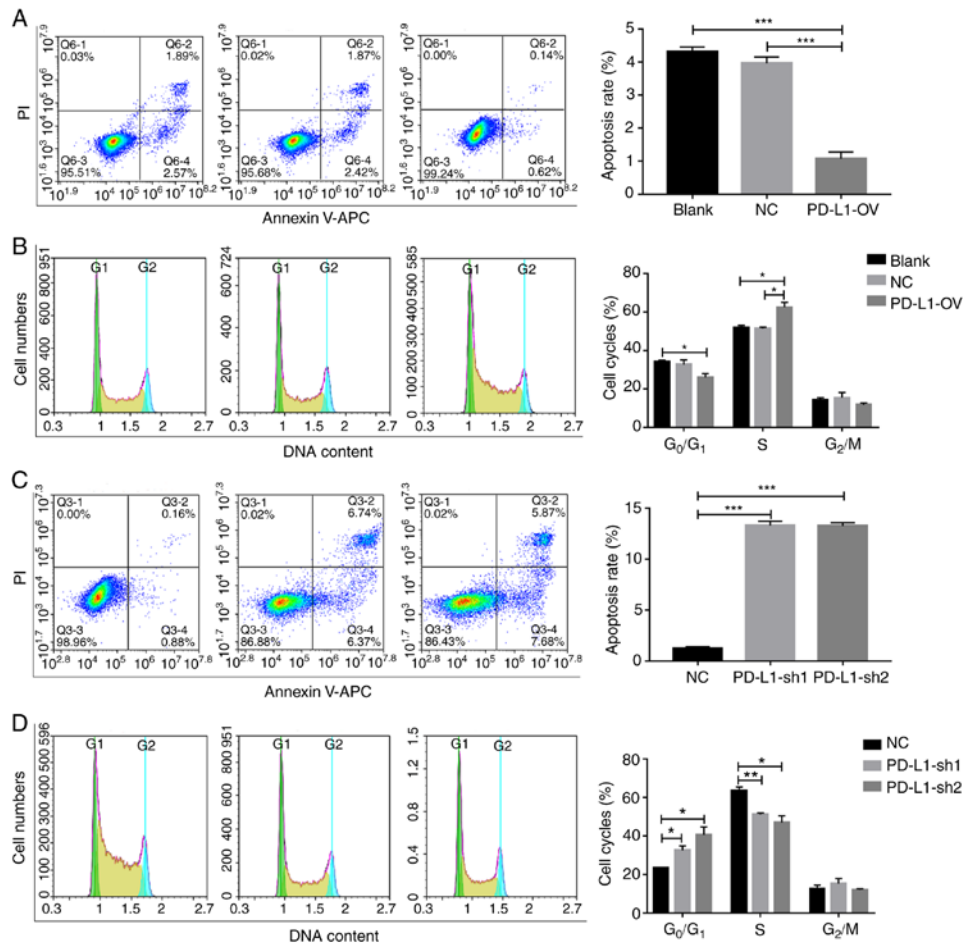


Figure 4. PD-L1 inhibits tumor cell apoptosis and promotes progression of cells into the S phase. (A and C) Cell apoptosis and (B and D) the cell cycle were detected by flow cytometry in MOLM-13 (Blank, NC and PD-L1-OV) and THP1 (NC and PD-L1-sh1/2) cell lines, respectively. Left, representative images of cell apoptosis and the cell cycle. Right, Statistical histograms. Data represent the results obtained from three independent experiments. * $P < 0.05$, ** $P < 0.01$ and *** $P < 0.001$. PD-L1, programmed cell death 1 ligand 1; PD-L1-OV, PD-L1 overexpressed.

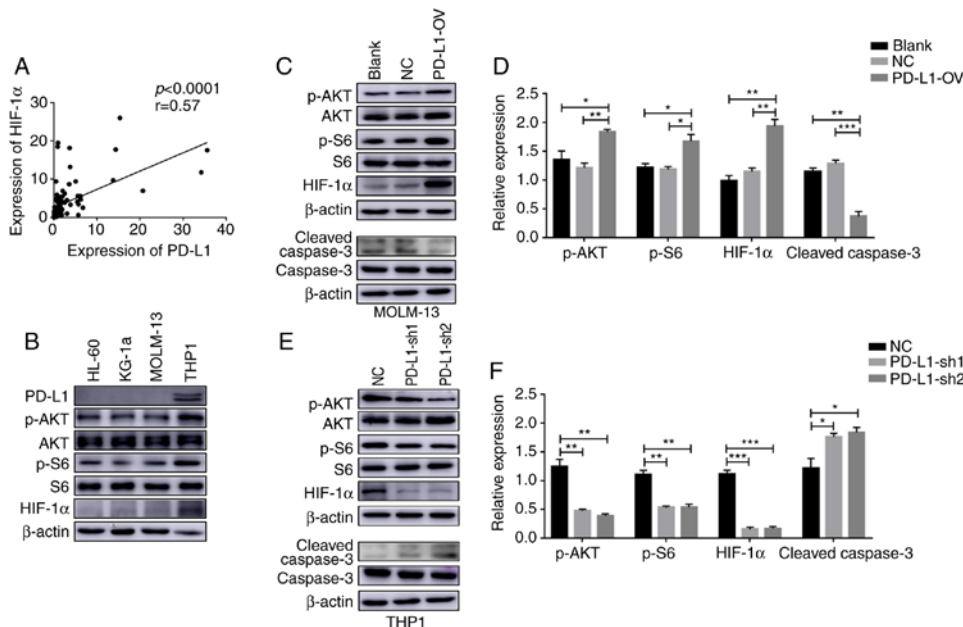


Figure 5. The Akt/mTOR/HIF-1α signaling pathway is regulated by PD-L1. (A) Correlation analysis of PD-L1 and HIF-1α were analyzed in patients with AML. (B) Expression of PD-L1 and Akt/S6/HIF-1α in four AML cell lines. (C and E) Representative images of phosphorylation of Akt and S6, HIF-1α and cleaved caspase-3 in MOLM-13, MOLM-13-NC, PD-L1-OV MOLM-13, THP1 and PD-L1-sh1/2 THP1 cell lines. (D and F) Statistical graphs of western blot assays. Data represent the results obtained from three independent experiments. * $P < 0.05$, ** $P < 0.01$ and *** $P < 0.001$. PD-L1, programmed cell death 1 ligand 1; AML, acute myeloid leukemia; PD-L1-OV, PD-L1 overexpressed.

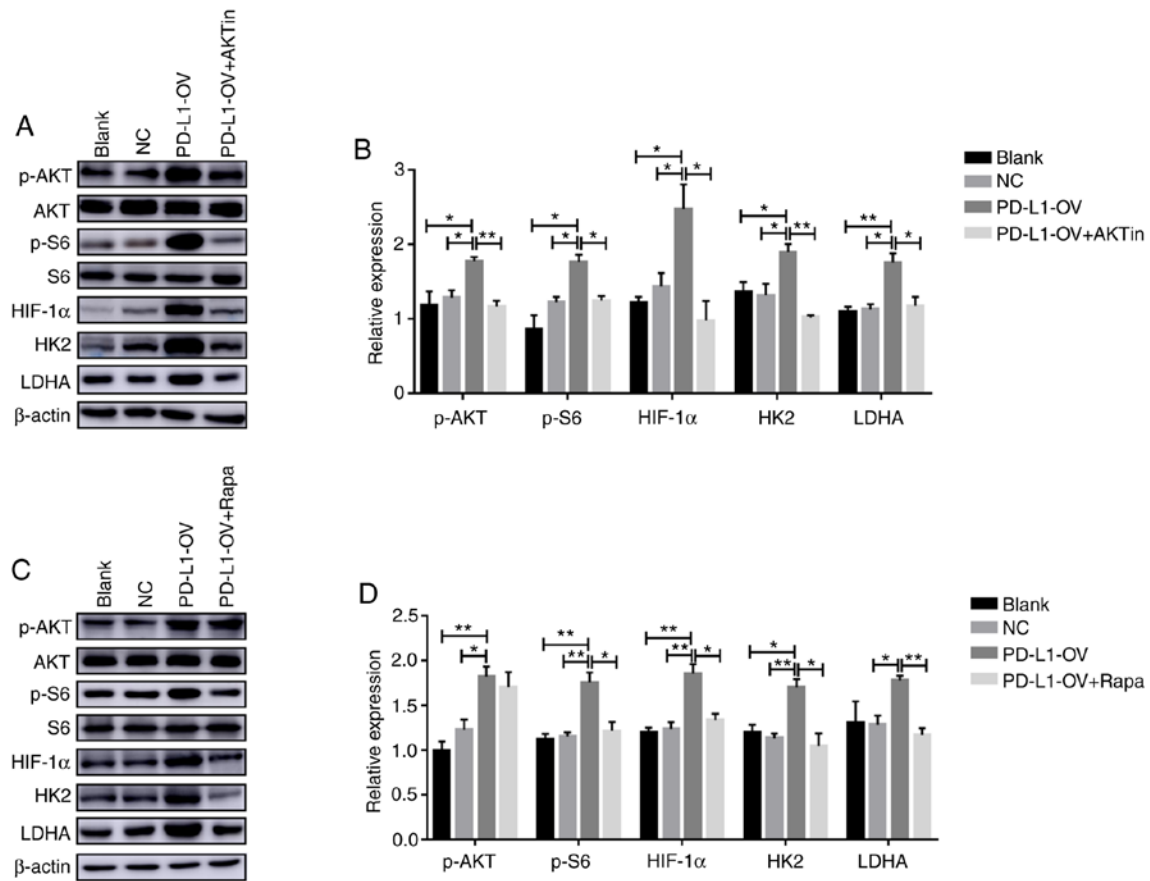


Figure 6. PD-L1 increases cell glycolysis via an Akt/mTOR/HIF-1α axis. Akt inhibitor and mTOR inhibitor rapamycin were added into cell medium to co-culture with PD-L1-OV MOLM-13 cells overnight. (A and C) The activation of Akt/mTOR/HIF-1α signaling and the expression of HK2 and LDHA were detected via western blotting. Data represent the results obtained from three independent experiments. (B and D) Statistical graphs of western blotting assays. *P<0.05, **P<0.01. PD-L1, programmed cell death 1 ligand 1; PD-L1-OV, PD-L1 overexpressed.

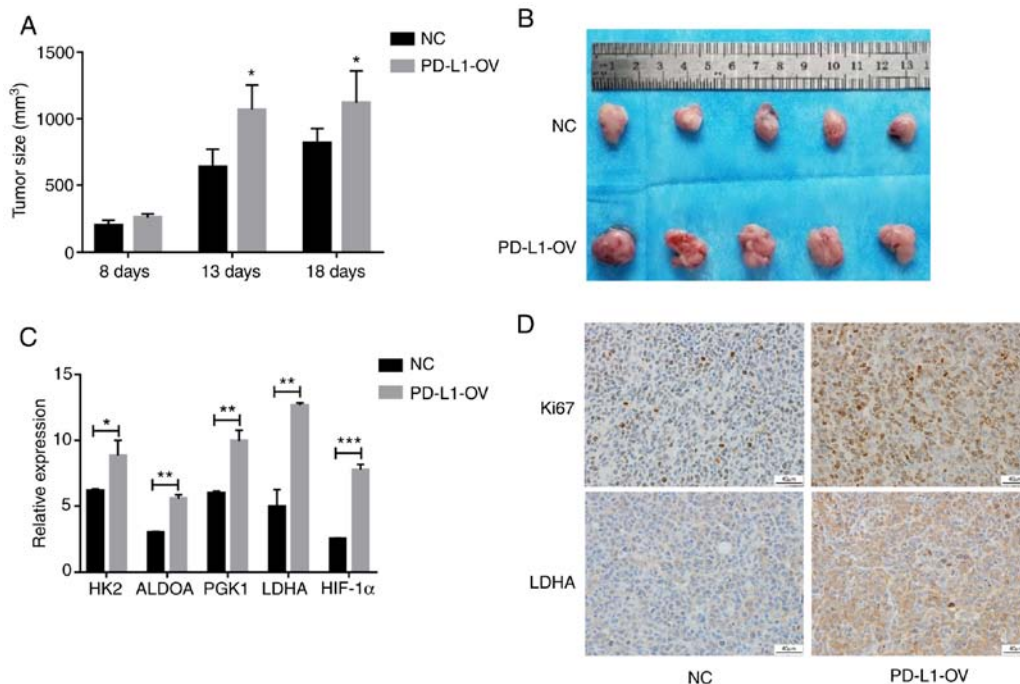


Figure 7. PD-L1 contributes to tumor progression and glycolysis *in vivo*. A total of 5x10⁶ PD-L1-OV MOLM-13 and NC MOLM-13 were injected subcutaneously into the right flank of each mouse. (A) The volume of tumors in the NC (n=5) and PD-L1-OV groups (n=5) at 8, 13 and 18 days. Mice with tumors were sacrificed at 18 days. (B) A representative image of tumors is presented. (C) Glycolysis-associated genes and HIF-1α expression in NC and PD-L1-OV groups were analyzed by RT-PCR. (D) The protein levels of Ki67 and LDHA were detected by IHC in tumor tissues. *P<0.05, **P<0.01 and ***P<0.001. PD-L1, programmed cell death 1 ligand 1; PD-L1-OV, PD-L1 overexpressed.

cells (44). The results of the present study coincided with previous research that revealed that Ki67 expression of tumor tissue in the PD-L1-OV MOLM13 group was higher than in the NC group in mouse models, indicating that PD-L1 plays a major role in regulating tumor growth. The molecular mechanism of the pro-tumor effect of PD-L1 is yet to be elucidated.

There have been a number of studies that have focused on the regulatory mechanism of glycolysis. It was investigated that glycolysis was regulated by the long non-coding RNA HOTTIP/ miR-615-3p/HMGB3 axis to impact tumor cell behaviors in non-small cell lung carcinoma (45). Another study revealed that glycolysis metabolism could be controlled by protein kinase C- α , due to the progression of non-small-cell lung carcinoma (46). PCK1 is another gene that participates in cell glycolysis metabolism. Chen and Zhu reported that Sonic Hedgehog upregulated cell glycolysis by promoting the phosphorylation of PI3K and Akt and induced the expression of PCK1 (47). In the present study, PD-L1-OV MOLM-13 cells were treated with Akt inhibitor and rapamycin, and it was revealed that glycolysis-associated proteins HK2 and LDHA were down-regulated. PD-L1 has been reported to enhance the proliferation and progression of tumor cells and trigger cell glycolysis through the mTOR signaling pathway in a mouse sarcoma model (21). Phosphorylation of Akt and S6 was enhanced following over-expression of PD-L1 in AML tumor cells in the present study. In the bone marrow microenvironment, oxygen pressure is physiologically lower than culture medium, which induced HIF-1 α (30). Although hypoxia was a significant prognostic factor in solid tumors, the conclusions of blood tumors, such as AML, were similar (2). In addition, it was also revealed that PD-L1 expression was positively correlated with HIF-1 α both in the present study and in publicly available data and HIF-1 α expression was affected by Akt/mTOR signaling. Therefore, it was speculated that HIF-1 α impacted by Akt/mTOR signaling could control AML cell glycolysis and it would be further identified that HIF-1 α directly regulates glycolysis-associated genes in future research. In addition, due to the lack of knowledge regarding the signaling motif and signaling transduction of PD-L1, RNA-sequencing of NC and PD-L1-OV cell lines will be performed our future study, for further analysis to identify the signal molecules involved in signaling transduction.

In conclusion, high PD-L1 expression was associated with high expression of glycolysis-associated genes and poor prognosis in patients with AML. The present study investigated and elucidated an important regulatory mechanism of PD-L1 in AML cell lines. PD-L1 increased glycolysis metabolism through Akt/mTOR/HIF-1 α signaling, leading to rapid cell proliferation and progression. Based on these findings, PD-L1 may be considered as a suitable marker for prognosis and treatment in a clinical setting.

Acknowledgements

We thank Henan Key Laboratory for Pharmacology of liver diseases for their animal experiment support.

Funding

The present study was supported by grants from the National Natural Science Foundation of China (81800104).

Availability of data and materials

The data generated, used and analyzed in the current study are available from the corresponding author in response to reasonable request.

Authors' contributions

LS conceived and supervised this study. PM and MX designed and conducted the research. LH, SG, JM, FW, YH, YC, WT, CA and HS participated in this project and helped to analyze the data. All authors read and approved the manuscript and agree to be accountable for all aspects of the research in ensuring that the accuracy or integrity of any part of the work are appropriately investigated and resolved.

Ethics approval and consent to participate

Ethical approval was obtained from the Human Research Ethics Committee (First Affiliated Hospital of Zhengzhou University, China). All patients provided written informed consent. The experiments involving mice were approved by the Institutional Animal Care and Use committee of the First Affiliated Hospital of Zhengzhou University.

Patient consent for publication

Not applicable.

Conflict of interests

The authors declare that they have no conflict of interest.

References

1. Liu Y, Lu R, Cui W, Pang Y, Liu C, Cui L, Qian T, Quan L, Dai Y, Jiao Y, *et al*: High IFITM3 expression predicts adverse prognosis in acute myeloid leukemia. *Cancer Gene Ther*: Mar 29, 2019 (Epub ahead of print).
2. Jabari M, Allahbakhshian Farsani M, Salari S, Hamidpour M, Amiri V and Mohammadi MH: Hypoxia-inducible Factor-1A (HIF1a) and vascular endothelial growth Factor-A (VEGF-A) expression in de novo AML patients. *Asian Pac J Cancer Prev* 20: 705-710, 2019.
3. Winer ES and Stone RM: Novel therapy in Acute myeloid leukemia (AML): Moving toward targeted approaches. *Ther Adv Hematol* 10: 2040620719860645, 2019.
4. Percival MM and Estey EH: Current treatment strategies for measurable residual disease in patients with acute myeloid leukemia. *Cancer* 125: 3121-3130, 2019.
5. Yang X, Pang Y, Zhang J, Shi J, Zhang X, Zhang G, Yang S, Wang J, Hu K, Wang J, *et al*: High Expression levels of ACTN1 and ACTN3 indicate unfavorable prognosis in acute myeloid leukemia. *J Cancer* 10: 4286-4292, 2019.
6. Yohe S: Molecular genetic markers in acute myeloid leukemia. *J Clin Med* 4: 460-478, 2015.
7. Mender JH, Maharry K, Radmacher MD, Mrózek K, Becker H, Metzeler KH, Schwind S, Whitman SP, Khalife J, Kohlschmidt J, *et al*: RUNX1 mutations are associated with poor outcome in younger and older patients with cytogenetically normal acute myeloid leukemia and with distinct gene and MicroRNA expression signatures. *J Clin Oncol* 30: 3109-3118, 2012.
8. Ribas A and Wolchok JD: Cancer immunotherapy using checkpoint blockade. *Science* 359: 1350-1355, 2018.
9. Zou W and Chen L: Inhibitory B7-family molecules in the tumour microenvironment. *Nat Rev Immunol* 8: 467-477, 2008.

10. Li H, Wang Z, Zhang Y, Sun G, Ding B, Yan L, Liu H, Guan W, Hu Z, Wang S, *et al*: The immune checkpoint regulator PDL1 is an independent prognostic biomarker for biochemical recurrence in prostate cancer patients following adjuvant hormonal therapy. *J Cancer* 10: 3102-3111, 2019.
11. Gato-Cañás M, Zuazo M, Arasanz H, Ibañez-Vea M, Lorenzo L, Fernandez-Hinojal G, Vera R, Smerdou C, Martisova E, Arozarena I, *et al*: PDL1 signals through conserved sequence motifs to overcome interferon-mediated cytotoxicity. *Cell Rep* 20: 1818-1829, 2017.
12. Bertucci F, Finetti P, Perrot D, Leroux A, Collin F, Le Cesne A, Coindre JM, Blay JY, Birnbaum D and Mameessier E: PDL1 expression is a poor-prognosis factor in soft-tissue sarcomas. *Oncoimmunology* 6: e1278100, 2017.
13. Yoyen-Ermis D, Tunali G, Tavukcuoglu E, Horzum U, Ozkazanc D, Sutlu T, Buyukaski Y and Esendagli G: Myeloid maturation potentiates STAT3-mediated atypical IFN- γ signaling and upregulation of PD-1 ligands in AML and MDS. *Sci Rep* 9: 11697, 2019.
14. Mussetti A, Pellegrinelli A, Cieri N, Garzone G, Dominoni F, Cabras A and Montefusco V: PD-L1, LAG3, and HLA-DR are increasingly expressed during smoldering myeloma progression. *Ann Hematol* 98: 1713-1720, 2019.
15. Zerdes I, Matikas A, Bergh J, Rassidakis GZ and Foukakis T: Genetic, transcriptional and post-translational regulation of the programmed death protein ligand 1 in cancer: Biology and clinical correlations. *Oncogene* 37: 4639-4661, 2018.
16. Pavlova NN and Thompson CB: The emerging hallmarks of cancer metabolism. *Cell Metab* 23: 27-47, 2016.
17. Ma J, Liu B, Yu D, Zuo Y, Cai R, Yang J and Cheng J: SIRT3 deacetylase activity confers chemoresistance in AML via regulation of mitochondrial oxidative phosphorylation. *Br J Haematol* 187: 49-64, 2019.
18. Gregory MA, Nemkov T, Park HJ, Zaberezhnyy V, Gehrke S, Adane B, Jordan CT, Hansen KC, D'Alessandro A and DeGregori J: Targeting glutamine metabolism and redox state for leukemia therapy. *Clin Cancer Res* 25: 4079-4090, 2019.
19. Boussiotis VA: Molecular and biochemical aspects of the PD-1 checkpoint pathway. *N Engl J Med* 375: 1767-1778, 2016.
20. Azuma T, Yao S, Zhu G, Flies AS, Flies SJ and Chen L: B7-H1 is a ubiquitous antiapoptotic receptor on cancer cells. *Blood* 111: 3635-3643, 2008.
21. Chang CH, Qiu J, O'Sullivan D, Buck MD, Noguchi T, Curtis JD, Chen Q, Gindin M, Gubin MM, van der Windt GJ, *et al*: Metabolic competition in the tumor microenvironment is a driver of cancer progression. *Cell* 162: 1229-1241, 2015.
22. Poulain L, Sujobert P, Zylbersztejn F, Barreau S, Stuanil L, Lambert M, Palama TL, Chesnais V, Birsén R, Vergez F, *et al*: High mTORC1 activity drives glycolysis addiction and sensitivity to G6PD inhibition in acute myeloid leukemia cells. *Leukemia* 31: 2326-2335, 2017.
23. Qian S, Li J, Hong M, Zhu Y, Zhao H, Xie Y, Huang J, Lian Y, Li Y, Wang S, *et al*: TIGAR cooperated with glycolysis to inhibit the apoptosis of leukemia cells and associated with poor prognosis in patients with cytogenetically normal acute myeloid leukemia. *J Hematol Oncol* 9: 128, 2016.
24. Cascone T, McKenzie JA, Mbofung RM, Punt S, Wang Z, Xu C, Williams LJ, Wang Z, Bristow CA, Carugo A, *et al*: Increased tumor glycolysis characterizes immune resistance to adoptive T cell therapy. *Cell Metab* 27: 977-987.e4, 2018.
25. Livak KJ and Schmittgen TD: Analysis of relative gene expression data using real-time quantitative PCR and the 2(-Delta Delta C(T)) method. *Methods* 25: 402-408, 2001.
26. Liu CC, Wang H, Wang WD, Wang L, Liu WJ, Wang JH, Geng QR and Lu Y: ENO2 promotes cell proliferation, glycolysis, and glucocorticoid-resistance in acute lymphoblastic leukemia. *Cell Physiol Biochem* 46: 1525-1535, 2018.
27. Tang Z, Li C, Kang B, Gao G, Li C and Zhang Z: GEPIA: A web server for cancer and normal gene expression profiling and interactive analyses. *Nucleic Acids Res* 45: W98-W102, 2017.
28. Fan K, Fan Z, Cheng H, Huang Q, Yang C, Jin K, Luo G, Yu X and Liu C: Hexokinase 2 dimerization and interaction with voltage-dependent anion channel promoted resistance to cell apoptosis induced by gemcitabine in pancreatic cancer. *Cancer Med* 8: 5903-5915, 2019.
29. Wang L, Shen S, Xiao H, Ding F, Wang M, Li G and Hu F: ARHGAP24 inhibits cell proliferation and cell cycle progression and induces apoptosis of lung cancer via a STAT6-WWP2-P27 axis. *Carcinogenesis*: Aug 20, 2019 (Epub ahead of print).
30. Harrison JS, Rameshwar P, Chang V and Bandari P: Oxygen saturation in the bone marrow of healthy volunteers. *Blood* 99: 394, 2002.
31. Liu J, Ren Y, Hou Y, Zhang C, Wang B, Li X, Sun R and Liu J: Dihydroartemisinin induces endothelial cell autophagy through suppression of the Akt/mTOR pathway. *J Cancer* 10: 6057-6064, 2019.
32. Baccelli I, Gareau Y, Lehnertz B, Gingras S, Spinella JF, Corneau S, Mayotte N, Girard S, Frechette M, Blouin-Chagnon V, *et al*: Mubritinib targets the electron transport chain complex I and reveals the landscape of OXPHOS dependency in acute myeloid leukemia. *Cancer Cell* 36: 84-99.e8, 2019.
33. Pollyea DA, Stevens BM, Jones CL, Winters A, Pei S, Minhajuddin M, D'Alessandro A, Culp-Hill R, Riemondy KA, Gillen AE, *et al*: Venetoclax with azacitidine disrupts energy metabolism and targets leukemia stem cells in patients with acute myeloid leukemia. *Nat Med* 24: 1859-1866, 2018.
34. Xu M, Seneviratne AK and Schimmer AD: Phospholipid metabolism regulates AML growth and stemness. *Aging (Albany NY)* 11: 3895-3897, 2019.
35. Yang J, Ren B, Yang G, Wang H, Chen G, You L, Zhang T and Zhao Y: The enhancement of glycolysis regulates pancreatic cancer metastasis. *Cell Mol Life Sci*: Aug 20, 2019 (Epub ahead of print).
36. Yeung C, Gibson AE, Issaq SH, Oshima N, Baumgart JT, Edessa LD, Rai G, Urban DJ, Johnson MS, Benavides GA, *et al*: Targeting glycolysis through inhibition of lactate dehydrogenase impairs tumor growth in preclinical models of Ewing sarcoma. *Cancer Res* 79: 5060-5073, 2019.
37. Ban D, Hua S, Zhang W, Shen C, Miao X and Liu W: Costunolide reduces glycolysis-associated activation of hepatic stellate cells via inhibition of hexokinase-2. *Cell Mol Biol Lett* 24: 52, 2019.
38. Nakazato K, Mogushi K, Kayamori K, Tsuchiya M, Takahashi KI, Sumino J, Michi Y, Yoda T and Uzawa N: Glucose metabolism changes during the development and progression of oral tongue squamous cell carcinomas. *Oncol Lett* 18: 1372-1380, 2019.
39. Cui L, Cheng Z, Liu Y, Dai Y, Pang Y, Jiao Y, Ke X, Cui W, Zhang Q, Shi J and Fu L: Overexpression of PDK2 and PDK3 reflects poor prognosis in acute myeloid leukemia. *Cancer Gene Ther*: Dec 22, 2018 (Epub ahead of print).
40. Song K, Li M, Xu X, Xuan LI, Huang G and Liu Q: Resistance to chemotherapy is associated with altered glucose metabolism in acute myeloid leukemia. *Oncol Lett* 12: 334-342, 2016.
41. Wu Z, Zhang L, Peng J, Xu S, Zhou L, Lin Y, Wang Y, Lu J, Yin W and Lu J: Predictive and prognostic value of PDL1 protein expression in breast cancer patients in neoadjuvant setting. *Cancer Biol Ther* 20: 941-947, 2019.
42. Zheng A, Li F, Chen F, Zuo J, Wang L, Wang Y, Chen S, Xiao B and Tao Z: PD-L1 promotes head and neck squamous cell carcinoma cell growth through mTOR signaling. *Oncol Rep* 41: 2833-2843, 2019.
43. Li H, Li CW, Li X, Ding Q, Guo L, Liu S, Liu C, Lai CC, Hsu JM, Dong Q, *et al*: MET inhibitors promote liver tumor evasion of the immune response by stabilizing PDL1. *Gastroenterology* 156: 1849-1861.e13, 2019.
44. Sun J, Jiang W, Tian D, Guo Q and Shen Z: Icotinib inhibits the proliferation of hepatocellular carcinoma cells in vitro and in vivo dependently on EGFR activation and PDL1 expression. *Onco Targets Ther* 11: 8227-8237, 2018.
45. Shi J, Wang H, Feng W, Huang S, An J, Qiu Y and Wu K: Long non-coding RNA HOTTIP promotes hypoxia-induced glycolysis through targeting miR-615-3p/HMGB3 axis in non-small cell lung cancer cells. *Eur J Pharmacol* 862: 172615, 2019.
46. Liu L, Lei B, Wang L, Chang C, Yang H, Liu J, Huang G and Xie W: Protein kinase C- α -mediated glycolysis promotes non-small-cell lung cancer progression. *Onco Targets Ther* 12: 5835-5848, 2019.
47. Chen Y and Zhu W: Knockdown of the Sonic Hedgehog (SHH) gene inhibits proliferation of Hep3B and SMMC-7721 hepatocellular carcinoma cells via the PI3K/Akt/PCK1 signaling pathway. *Med Sci Monit* 25: 6023-6033, 2019.